Assessment of cardiovascular dynamics by pressure-area relations in pediatric patients with congenital heart disease

Hideaki Senzaki, MD[a]
Chen-Huan Chen, MD[b]
Satoshi Masutani, MD[a]
Mio Taketazu, MD[a]
Jun Kobayashi, MD[a]
Toshiki Kobayashi, MD[a]
Nozomu Sasaki, MD[a]
Haruhiko Asano, MD[c]
Shunei Kyo, MD[c]
Yuji Yokote, MD[c]

Objectives: It is particularly useful to separately quantify the ventricular contractility and loading conditions for a better understanding of the cardiovascular dynamics in congenital heart disease, where abnormalities in chamber and loading properties may coexist. Furthermore, ventricular contractility and loading conditions may alter independently or simultaneously with disease progression and therapeutic intervention. The objectives of the present study were (1) to test whether ventricular pressure-area analysis can provide such quantitation among patients with various forms of congenital heart disease, (2) to reveal basal cardiovascular interaction in congenital heart disease by means of pressure-area analysis, and (3) to test the feasibility of this method in a simplified and less invasive form to further enhance its clinical value.

Methods: We constructed pressure-area loops during caval occlusion by using transthoracic echocardiographic automated border detection combined with ventricular pressure recordings in 59 pediatric patients with congenital heart disease and in 7 normal control subjects.

Results: Area measurements obtained by automated border detection were highly reproducible, and area changes reflected volume changes. The pressure-area data provided load-independent measures of contractility, which were consistently increased by use of dobutamine ($P < .05$). End-systolic and arterial elastance individually quantified simultaneous changes in ventricular contractility and loading with milrinone infusion and predicted net cardiac performance. The pressure-area analysis better characterized the ventricular contractile states under a variety of loading conditions in congenital heart disease, whereas predominant load dependence of conventional indices confounded them. Furthermore, pressure-area relations were reasonably estimated from a single beat and from aortic pressure data during abdominal compression.

Conclusions: Pressure-area analysis should provide a useful modality with which to assess cardiovascular dynamics in pediatric patients with congenital heart disease in more detail and should thus help improve the management of patients with this disease.

From the Departments of Pediatric Cardiology[a] and Cardiovascular Surgery,[c] Saitama Heart Institute, Saitama Medical School Hospital, Saitama, Japan, and the Cardiovascular Research Center,[b] National Yang-Ming University, Taipei Veterans General Hospital, Taipei, Taiwan.

Supported by National Grant No. 8025127 from the Japan Society for the Promotion of Science (H.S.).

Received for publication Sept 25, 2000; accepted for publication Feb 26, 2001.

Address for reprints: Hideaki Senzaki, MD, Department of Pediatric Cardiology, Saitama Heart Institute, Saitama Medical School Hospital, 38 Morohongo, Moroyama, Saitama 350, Japan (E-mail: hsenzaki@saitama-med.ac.jp).

J Thorac Cardiovasc Surg 2001;122:535-47

0022-5223/2001 $35.00 + 0 **12/1/115424**

doi:10.1067/mtc.2001.115424

CHD

With recent improvements in surgical and catheter intervention, together with the explosion in pharmacologic treatment options for pediatric patients with congenital heart disease (CHD), there is a growing need for more accurate and detailed measurements of cardiac performance. Anatomic abnormalities in CHD are generally associated with volume

or pressure overloading (or both) of the pulmonary ventricle, systemic ventricle, or both.[1] Under some conditions, overloading of one ventricle causes underloading of the opposite ventricular chamber. Such loading abnormalities can profoundly affect ventricular chamber mechanics. Cyanosis superimposed on various loading conditions may further influence myocardial performance.[2] In addition to these baseline hemodynamic characteristics in CHD, pharmacologic, surgical, or catheter intervention often dramatically alters chamber loading, which may simultaneously accompany changes in chamber contractile function. Thus, for cardiovascular dynamics in CHD to be better understood, chamber contractility and ventricular loading conditions must be separately quantified. Traditional measures of ventricular function, such as ejection fraction (EF) or maximum rate of pressure rise (dP/dtmax), predominantly depend on loading factors, as well as contractility, thus falling short of this mark.

Ventricular pressure-volume (P-V) relations, in contrast, provide a characterization of pump performance that allows loading factors to be reasonably separated from ventricular properties.[3,4] Loading factors and ventricular properties can in turn be coupled to predict net cardiac performance and to evaluate ventricular energetics.[4-7] Despite its potential usefulness in assessing cardiovascular dynamics in CHD, application to pediatric patients with CHD has been hindered primarily because of technical difficulties encountered in measuring instantaneous ventricular volume. However, ventricular chamber area can now be measured instantaneously by means of echocardiography with automated border detection (ABD).[8,9] Area data can be combined with simultaneous pressure data to construct ventricular pressure-area (P-A) relations, potentially providing a method to assess cardiovascular function in a manner similar to that of P-V relations. Thus, in the present study, we tested the validity of P-A analysis in CHD that presented a diversity of ventricular morphology and loading conditions. We then analyzed cardiovascular dynamics in the various types of CHD by this method.

The other important aspect in the assessment of cardiovascular function, particularly in pediatric patients, is that the method should be reasonably simple and less invasive. Such methods allow data to be obtained with minimal risk or discomfort to the patient, permitting studies to be repeated more frequently and under various test conditions. We therefore tested whether a P-A coupling framework can be determined by using a single P-A loop or by noninvasive means by use of aortic pressure tracing combined with abdominal compression.

Accordingly, the objectives of the present study were (1) to test whether P-A relations can be used to assess cardiovascular dynamics in CHD in a way similar to that of P-V relations, (2) to reveal basal ventricular-vascular interaction in CHD by means of P-A analysis, and (3) to test the feasibility of more simplified and less invasive applications of this method.

Methods

Patients

Data were analyzed from 66 patients, of whom 7 had normal hearts and 59 had various forms of CHD. Patient ages ranged from 1 month to 16 years (mean, 4.3 ± 4.8 years). Control subjects were patients who had had Kawasaki disease and had normal electrocardiograms, coronary angiograms, and contrast ventriculography. Patient characteristics are provided in Table 1. Written informed consent was obtained from the parents of all patients, and the procedures were approved by The Saitama Medical School Committee on Clinical Investigation.

Procedures

After routine cardiac catheterization and before angiography/ventriculography, P-A relations for the systemic ventricle were constructed by simultaneously measuring ventricular chamber pressure and area both at rest and during varying preloads by means of transient inferior vena caval balloon obstruction. The balloon catheter used was a 6F catheter developed in our laboratory to minimize vascular injury in small children. Ventricular pressure was measured with a high-fidelity pressure transducer mounted on a 0.014F guide wire (RADI Medical Systems AB, Uppsala, Sweden) placed within a 4F or 5F pigtail catheter. Instantaneous ventricular cavity area was obtained by means of an ABD echocardiographic system[8,9] (Sonos 2500; Hewlett-Packard Company, Palo Alto, Calif) with a 3.5- or 5.5-MHz phased-array transducer. Transthoracic 2-dimensional images were recorded from the midventricular short-axis plane with the midpapillary muscle level used as an anatomic landmark. Overall transmit, time gain compensation, and lateral gain controls were adjusted by means of visual inspection as a compromise between cavity clutter and wall dropout. A region of interest was then drawn immediately beyond the endocardial border. The traced area within the region of interest was automatically calculated, providing a real-time area waveform. P-A data were digitalized at 500 Hz by a custom-designed data acquisition system and displayed in real time.

Data Analysis

Three to 5 consecutive steady-state beats were signal averaged and used to generate end-diastolic and end-systolic pressure, end-diastolic and end-systolic area, stroke area, area-based EF, dP/dtmax, and the effective arterial elastance (Ea), which is a lumped measure of ventricular afterload.[5,6] Arterial load presented to the heart should encompass both mean and pulsatile components. Although the aortic input impedance spectra defined in the frequency domain provide such information, it is very difficult to link such data with time-domain or P-V (area) measurements of ventricular function. In contrast, Ea shares common units with elastance measures of ventricular function and thus enables ventricular-arterial interactions to be easily evaluated, while incorporating both mean and pulsatile components of ventricular load provided by impedance spectra.[5,6]

Area data were normalized by the body surface area of the patients and expressed as area indexes (end-diastolic area index [EDAI], end-systolic area index [ESAI], and stroke area index [SAI]). EF was calculated as SAI/EDAI and Ea as end-systolic pressure/SAI. Data measured during varying preloads by means of transient inferior vena caval occlusion or abdominal compression were used to determine the end-systolic pressure-area relation (ESPAR). Heart rate generally changed little during preload change, but to further eliminate rate effects, only beats for which heart rate varied by less than 5% of baseline were used for analysis. Points of maximal pressure/(area-Ao), where Ao was the ESPAR area-axis intercept, were calculated for each beat in the series by using an iterative method to measure Ao.[10,11] Data were fit by orthogonal regression,[12] yielding an ESPAR slope (end-systolic elastance [Ees]) and intercept (Ao).

Validation of area measurements by ABD. We tested the reproducibility of area measurements in 34 randomly selected patients by comparing area data recorded at the beginning of the routine catheterization and those obtained during the P-A study. For 21 patients in whom the systemic ventricle had a single outflow into the aorta, changes in stroke area during inferior vena caval occlusion were compared with those in stroke volume that were simultaneously measured with a catheter-mounted electromagnetic flow probe (Millar Instruments, Inc, Houston, Tex). This procedure tested whether area changes adequately reflected volume changes. The catheter was advanced retrogradely across the aortic valve to help stabilize it and to keep the sensor in the center of the stream. Ascending aortic cross-sectional area obtained from 2-dimensional echocardiograms was used to convert flow velocity to volume flow.

Contractility response to a positive inotrope. To determine whether P-A loops and relations adequately reflect changes in contractility in response to a positive inotrope, changes in ESPAR, the slope of dP/dtmax-EDAI relation,[13] and the slope of stroke work index (SWI)-EDAI relation[14] were compared before and after the administration of dobutamine (5-15 $\mu g \cdot kg^{-1} \cdot min^{-1}$) in 27 patients (4 patients with Kawasaki disease, 5 with ventricular septal defect, 3 with patent ductus arteriosus, 3 with atrial septal defect, 3 with pulmonary stenosis, 3 with coarctation of the aorta, 4 with single ventricle, and 2 with dilated cardiomyopathy). The latter 2 indices can be obtained from the same set of P-A data and have proven to provide relatively load-insensitive measure of contractility in P-V analysis.[4,13,14]

Ventricular-vascular coupling. We further tested the ability of P-A loops and relations to independently quantify changes in ventricular performance and vascular loading when simultaneous changes in contractility and arterial load occur. In 17 patients (3 with Kawasaki disease, 4 with ventricular septal defect, 2 with patent ductus arteriosus, 2 with coarctation of the aorta, 2 with atrial septal defect, 2 with pulmonary stenosis, and 2 with single ventricle), the P-A relation was analyzed during an intravenous injection of milrinone, an agent that has both positive inotropic and vasodilating effects.

Once determined, Ees and Ea can be combined in a coupling relation to predict EF (Appendix 1):

$$EF = SAI/EDAI = Ees\,[1 - (Ao/EDAI)]/(Ea + Ees).$$

This equation indicates that EF can be predicted as a function of changes in preload (EDAI), afterload (Ea), and ventricular contractile state (Ees and Ao). Thus, to better test the validity and usefulness of the P-A coupling framework in assessing cardiovascular dynamics in CHD, we compared predicted and directly calculated EF.

TABLE 1. Patient characteristics

Diagnosis	No. of patients	Age (y)
Kawasaki disease	7	5.3 ± 5.0
VSD (2 had significant MR)	16	3.3 ± 3.6
CoA	5	2.5 ± 4.2
PDA	5	2.6 ± 2.4
ASD	6	11 ± 6.2
PS	6	3.7 ± 4.4
AVSD	3	0.8 ± 0.7
S/P Fontan operation	4	10.8 ± 5.0
SiV	7	1.7 ± 1.7
DCM	3	9.5 ± 3.5
Others	4	3.9 ± 5.4
Total	66	4.3 ± 4.8

VSD, Ventricular septal defect; *MR*, mitral regurgitation; *CoA,* coarctation of the aorta; *PDA,* patent ductus arteriosus; *ASD,* atrial septal defect; *PS,* pulmonary stenosis; *AVSD*, atrioventricular septal defect; *S/P*, status post; *SiV,* single ventricle; *DCM,* dilated cardiomyopathy.

Basal cardiovascular dynamics of CHD. P-A loops and relations were then used to assess cardiovascular interaction in various forms of CHD. Four groups of patients with hemodynamically representative CHD were studied: left ventricular (LV) volume overload (ventricular septal defect); LV pressure overload (coarctation of the aorta); right ventricular (RV) volume overload (atrial septal defect); and RV pressure overload (pulmonary stenosis). LV Ees, Ea, and their coupling ratios were compared in association with other hemodynamic variables.

Estimation of ESPAR from a single beat. To determine ESPAR and thus its coupling with vascular load, multiple P-A loops with different loading conditions must be generated. This limits its applicability, particularly in the clinical setting. Estimation of ESPAR from a single P-A loop would therefore enhance its clinical value. Methods for estimating single-beat end-systolic pressure-volume relation (ESPVR) have been proposed by others,[15,16] as well as by us.[12] We tested whether the same method can be applied to P-A loops to obtain ESPAR from a single beat.

The method proposed by Senzaki and colleagues[12] is based on normalized time-varying elastance curves ($E_N[t_N]$; Appendix 2). Our finding that $E_N(t_N)$ curves in adult human beings were remarkably consistent despite variations in underlying cardiac disease, contractility, loading, and heart rate enables ESPVR to be estimated from one beat with a known value of $E_N(t_N)$ at a given t_N (normalized time). Accordingly, we first tested whether $E_N(t_N)$ curves were consistent among patients with a wide spectrum of CHD (Appendix 2). Once the standard $E_N(t_N)$ curve was determined, Ao and thus Ees were calculated by using a known $E_N(t_N)$ value and pressure and area measured at a selected t_N (Appendix 3). This Ees is referred to as $Ees(E_N)$.

An alternative method, originally proposed by Sunagawa and colleagues,[15] assumes linear ESPVR and mathematically predicts peak isovolumic pressure (P_{iso}) by curve fitting isovolumic data

CHD

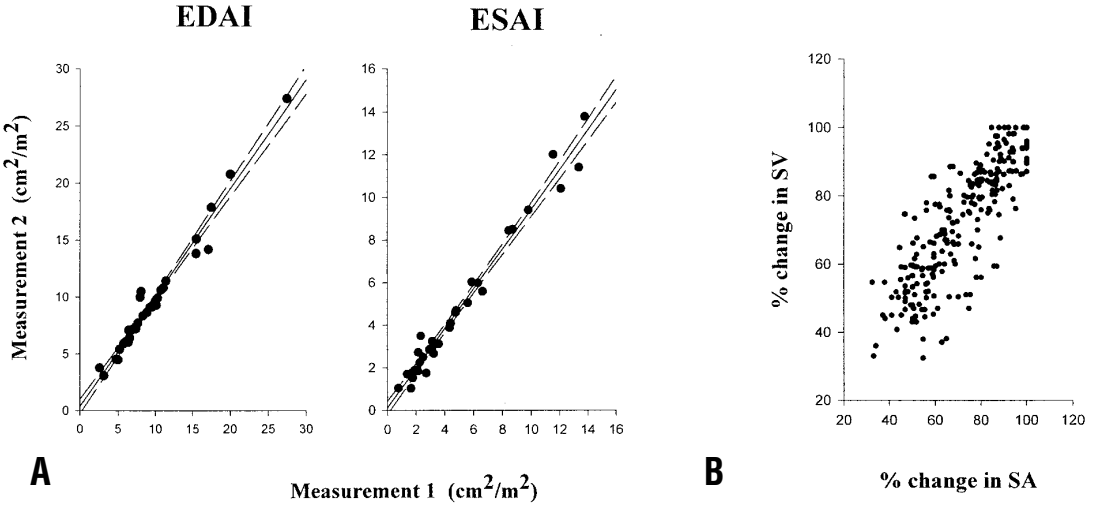

Figure 1. A, Relation between the measurements of EDAI and ESAI repeated on 2 separate occasions. Linear regression is shown as solid lines; dashed lines indicate 95% confidence intervals. B, Relation of changes in stroke area (SA) to simultaneously measured changes in stroke volume (SV) during inferior vena caval occlusion.

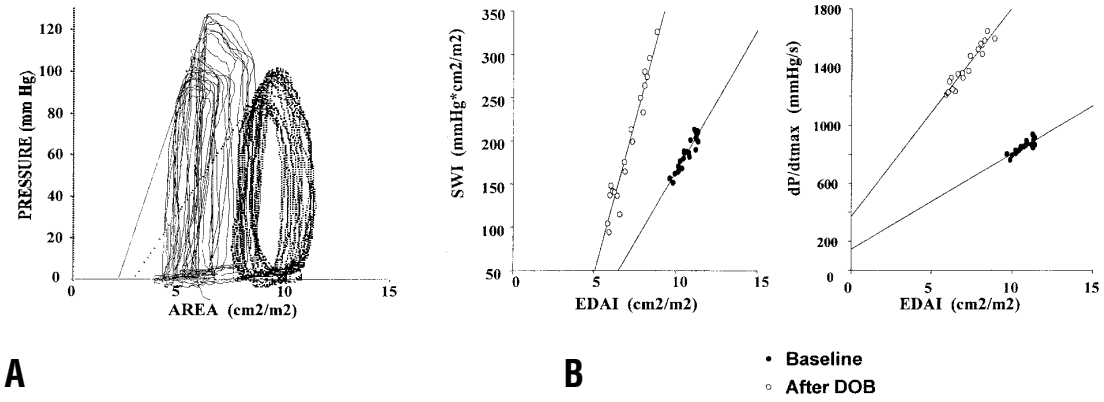

Figure 2. Contractile response to dobutamine. A, P-A loops and end-systolic P-A relations before (dotted lines) and after (solid lines) dobutamine (DOB) infusion. End-systolic elastance increased from 17.1 to 36.6 mm Hg · m^2 · cm^{-2}. B, Relations between SWI versus EDAI and between dP/dtmax versus EDAI obtained from the same set of P-A data in A. Baseline relations are shown by filled circles, and relations after dobutamine infusion are shown by open circles.

from an ejection beat to cosine function, yielding Ees from a single beat (Ees[iso]; Appendix 4).

Both Ees(E_N) and Ees(iso) were compared with the multiple beat–derived Ees value (Ees[MB]).

Noninvasive application. Combining aortic pressure and ventricular area data, a P-A loop can be constructed during the ejection period. Ventricular preload can be noninvasively altered by abdominal compression to change venous return,[17] and thus ESPAR and its coupling to Ea can be estimated by noninvasive means. To test the feasibility of this method, we compared Ees derived from LV pressure during inferior vena caval occlusion (Ees[LV]) and aortic pressure-based Ees obtained during abdominal compression (Ees[AO]) in a random subset of 28 patients. Data were compared both at rest and after increased contractility caused by administration of dobutamine.

Statistics

Data are presented as means ± standard deviation. The correlation between 2 variables was tested by means of linear regression analysis. Effects of dobutamine on contractile indices and the effects of milrinone on Ees and Ea were tested by means of multivariate regression analysis.

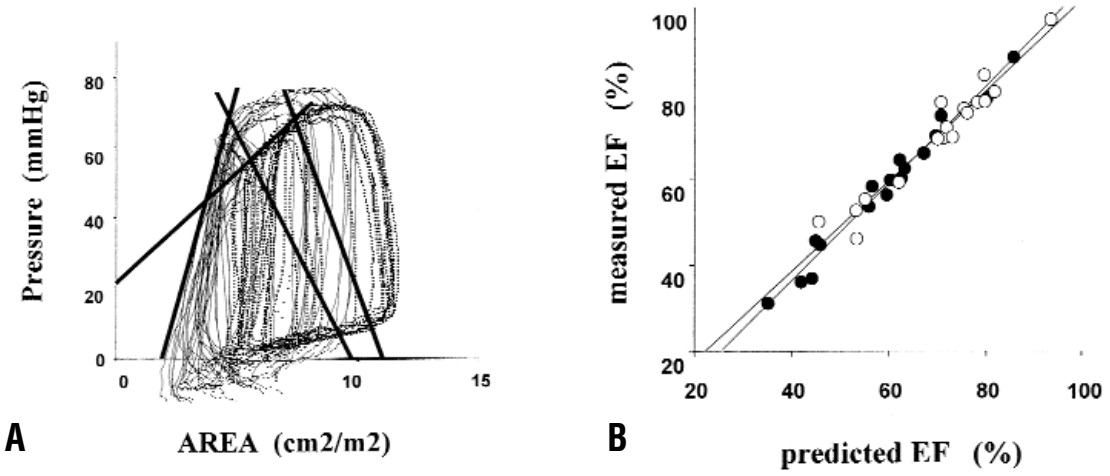

Figure 3. A, Example P-A data before and after acute changes in ventricular contractility and afterload with milrinone. P-A loops at baseline and after milrinone infusion are shown by *dotted* and *solid lines,* respectively. End-systolic P-A relations and arterial elastance in each condition are in bold. B, Relationship between predicted EF by the coupling framework model and measured EF both at rest *(filled circles)* and after milrinone infusion *(open circles).*

Results

Validation of Area Measurements by ABD

Figure 1, *A*, displays scatter plots of the measurements of ventricular areas repeated on 2 separate occasions. Two patients with a heart rate change of greater than 10 beats/min were excluded. The plots show good correlation with little variability (EDAI: y = 0.98x + 0.28, $r = 0.99$, and standard error of the estimate [SEE] = 0.69; ESAI: y = 1.0x + 0.1, $r = 0.99$, and SEE = 0.44; both $P < .0001$). Figure 1, *B*, shows pooled data describing the relationship between stroke area and stroke volume change during inferior vena caval occlusion. Variables are plotted, with 100% representing baseline values before inferior vena caval occlusion. The relationship between the variables was predominantly linear ($r = 0.88 \pm 0.08$, SEE = 8% ± 4%), with a regression slope of 0.90 ± 0.18. Five patients with atrial septal defect who showed paradoxical septal motion were included in these studies, and their results were not different from those of the remaining patients, indicating that the effects of paradoxical septal motion on the accuracy of the area measurements and the relationship to stroke volume are minimal. Thus, ventricular area measurements by ABD from the transthoracic approach provided reproducible data and accurately reflected ventricular volume change.

Contractility Response to a Positive Inotrope

Figure 2, *A*, displays example plots of P-A loops and relations before and after dobutamine infusion in a patient with a functional single ventricle after a Fontan operation. The patient had a double-outlet right ventricle, tricuspid and mitral valve regurgitation, and multiple ventricular septal defects, including a restrictive perimembranous defect with straddling tricuspid valves. P-A analysis for this complicated ventricle yielded a predominant linear ESPAR that shifted leftward with increased slope after dobutamine infusion, which is consistent with increased chamber contractility. Figure 2, *B*, shows the changes in SWI-EDAI and dP/dtmax-EDAI relations obtained from the same set of P-A loops. The linear regression slopes of each relation increased with dobutamine administration, which is consistent with changes in ESPAR (increased contractility). Multivariate regression analysis of data from all patients revealed a significant increase in all 3 variables with dobutamine administration (Ees: 14.1 ± 3.7 to 37.7 ± 19.6 mm Hg $\cdot$ m^2 $\cdot$ cm^{-2}; Ao: –2.7 ± 2.1 to –0.78 ± 2.4 cm^2/m^2; SWI-EDAI: 55.8 ± 14.8 to 104.9 ± 26.2 mm Hg; dP/dtmax-EDAI: 123.9 ± 68.1 to 352.4 ± 248.2 mm Hg $\cdot$ m^{-2} $\cdot$ s^{-1} $\cdot$ cm^{-2}; all $P < .001$). To confirm that changes in these indices are due to true alterations in ventricular contractility but not due to their variability, reproducibility of each index was tested under steady-state conditions. Measurements showed little variability with coefficients of variation (SD/mean × 100) of 8.6% ± 4.9% for Ees, 3.8% ± 2.5% for stroke work–end-diastolic area relation, and 9.8% ± 5.3% for dP/dtmax–end-diastolic area relation. Thus, P-A loops and relations provide load-insensitive contractility indices in patients with various forms of CHD, as do P-V relations.

Ventricular-Vascular Coupling Framework

Figure 3, *A*, displays an example set of P-A loops and changes in ESPAR and Ea before and after milrinone infusion in a patient with a patent ductus arteriosus. The Ees increased with a concomitant decrease in Ea. Group Ees

CHD

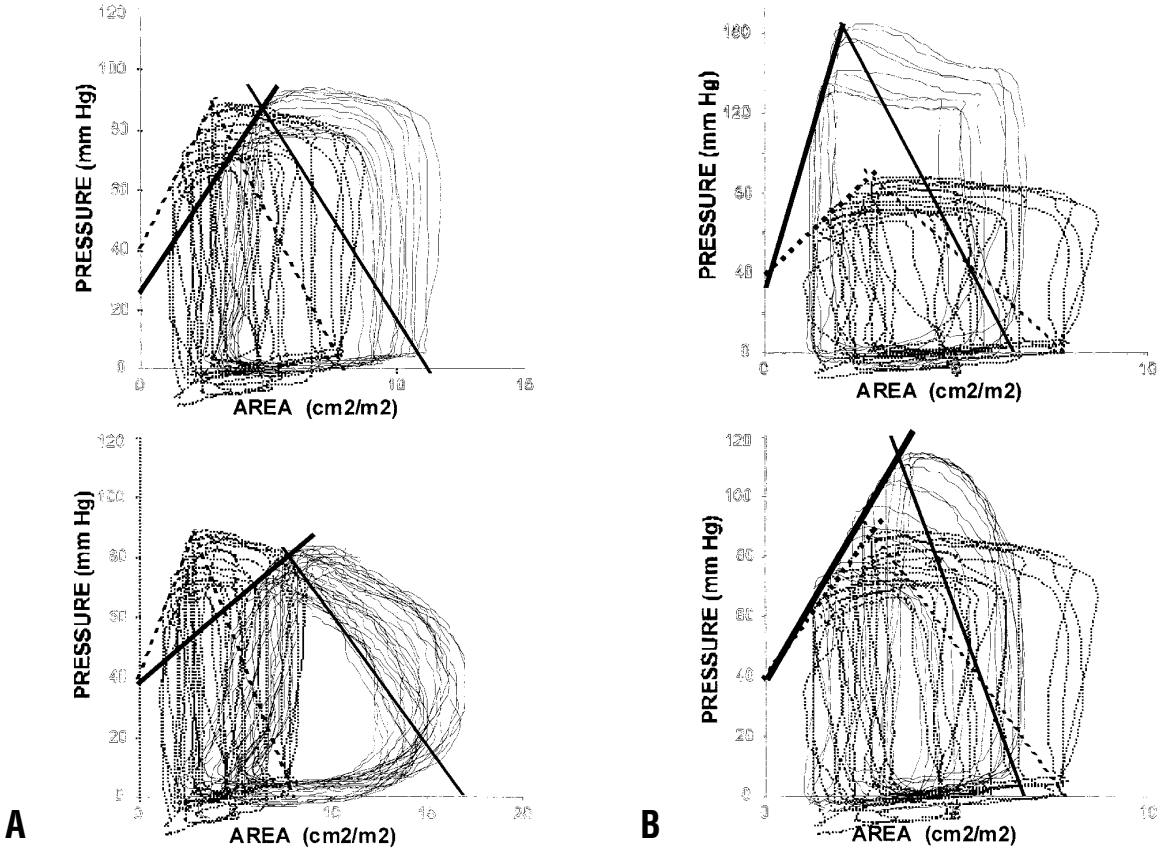

Figure 4. Example plots of P-A data in CHD *(solid lines).* Data from a representative normal control subject are reproduced in each panel to assist comparison *(dotted lines).* A, Data from patients with a ventricular septal defect (VSD) in which pulmonary/systemic blood flow ratios (Qp/Qs) were 1.8 (upper panels) and 2.9 (lower panels). B, Data from patients with coarctation of the aorta (CoA). The patient shown in the upper panel had 50 mm Hg of pressure gradient (ΔP) across the coarctation but no heart failure symptoms, and the patient in the lower panel manifested heart failure symptoms with ΔP of 30 mm Hg.

increased from 15.5 ± 8.0 to 28.6 ± 13.1 mm Hg · cm^{-2} · m^2 (Ao from –2.7 ± 2.1 to –0.8 ± 2.4 cm^2/m^2, $P = .02$ by means of a paired *t* test), and Ea decreased from 26.5 ± 11.1 to 22.3 ± 10.3 mm Hg · cm^{-2} · m^2 (both $P < .001$ by means of a paired *t* test). These changes were independent of CHD type ($P < .01$ by means of multivariate regression analysis), suggesting that simultaneous changes in ventricular contractility and vascular loading condition can be separately quantified by P-A relations in CHD. Changes in Ees and Ea were in turn coupled to predict the net change in ventricular performance (Figure 3, *B*). The ventricular-vascular coupling model based on Ees and Ea changes derived from P-A loops precisely predicted changes in EF caused by milrinone infusion ($r = 0.98$ before and after milrinone, $P < .001$).

Baseline Ventricular-Vascular Interaction in CHD

Figure 4 displays example plots of P-A loops and relations in various forms of CHD. The P-A relations of a representative normal control subject are reproduced in each panel by *dotted lines* to assist comparison. The heart rate, EF, and dP/dtmax values for this patient were 110 beats/min, 69%, and 1540 mm Hg/s, respectively. In each disease 2 conditions are shown in the *upper* and *lower panels.* Summary data are also presented in Table 2. The Ees and Ea values in normal children were 21.8 ± 7.4 and 24.4 ± 8.2 mm Hg · cm^{-2} · m^2, respectively, and their coupling ratios were maintained within a relatively small range (0.91 ± 0.21).

P-A loops in patients with a ventricular septal defect (Figure 4, *A*) were characterized by increased EDAI and decreased Ea (both $P = .01$ vs control subjects), which were more pronounced with a large left-to-right shunt *(lower panel).* The LV contractile state of ventricular septal defect was also dependent on the amount of shunt, with lower Ees associated with a high pulmonary/systemic flow ratio (Qp/Qs; Ees = –3.0 Qp/Qs + 18.5, $r = 0.61$, $P < .01$). Although EF or dP/dtmax values were similar to those of normal patients ($P =$

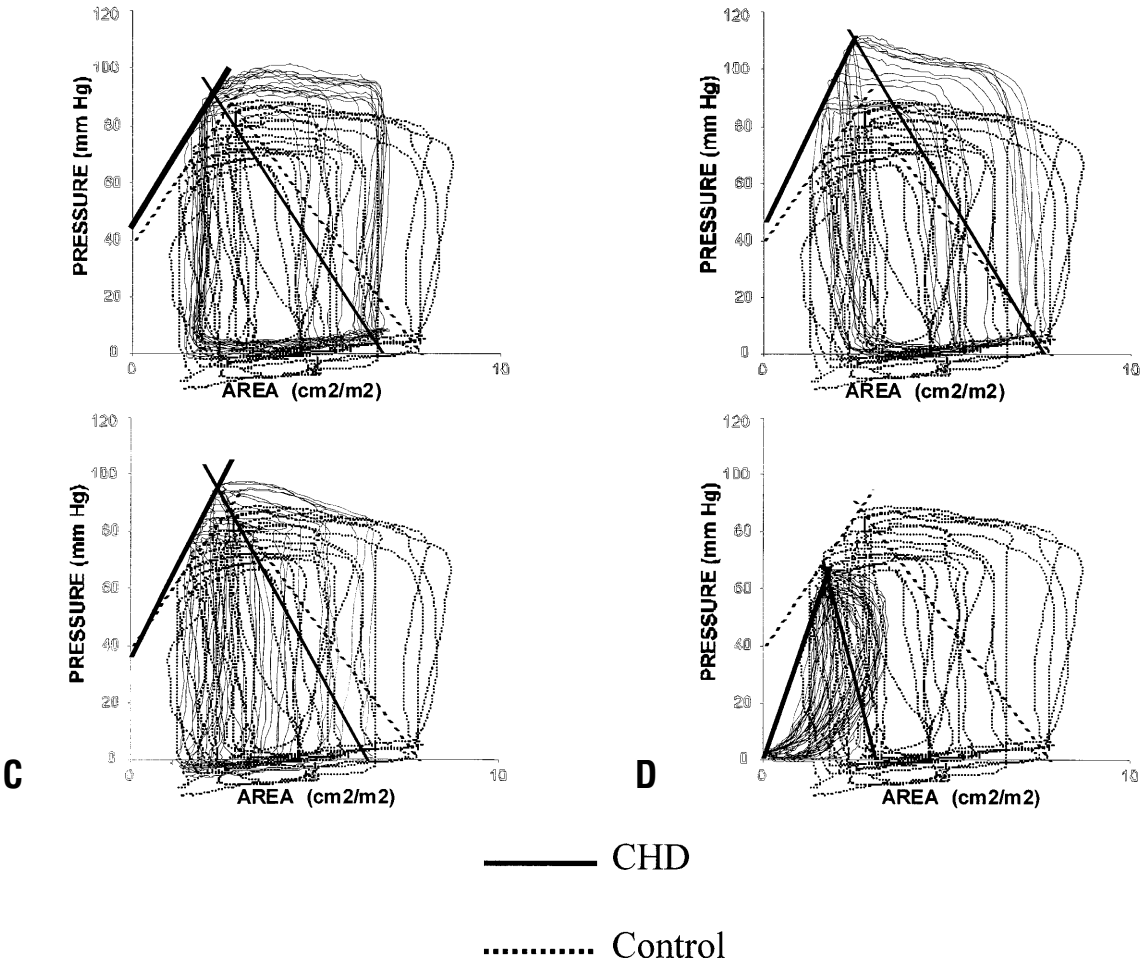

Figure 4. Cont'd. C, Atrial septal defect (ASD) in which Qp/Qs values were 1.6 (upper panel) and 2.4 (lower panel). D, Pulmonary stenosis (PS) in which ΔP was 38 mm Hg (upper panel) and 60 mm Hg (lower panel). The patient in the upper panel was asymptomatic, whereas the patient in the lower panel manifested overt heart failure with right-to-left shunt through a foramen ovale.

.68 for EF and $P = .45$ for dP/dtmax), ventricular contractility as represented by Ees or the slope of SWI-EDAI relation was significantly lower than normal (both $P < .01$).

Increased afterload caused by coarctation of the aorta was characterized by increased Ea ($P < .01$ vs control subjects). The LV contractility (Ees) was markedly enhanced in response to chronically increased afterload in a 10-year-old patient, whose data are presented in the *upper panel.* This patient had no symptoms of heart failure. The resultant coupling ratio was slightly higher than normal, yielding a preserved stroke area despite a decreased EDAI and increased afterload. Of note, dP/dtmax of this patient was 1520 mm Hg/s and thus failed to detect increased contractile state. In contrast, P-A data from a 3-month-old infant who manifested overt heart failure *(lower panel)* revealed a minimal increase in Ees against increased Ea, which is consistent with afterload mismatch. This resulted in decreased stroke area and EF compared with those of normal control subjects. Of 5 patients with coarctation, 3 presented symptoms of heart failure, and their Ees values were significantly lower than those of the rest of the patients (18.9 ± 2.0 vs 38.2 ± 6.4 mm Hg · m^2 · cm^{-2}, $P < .01$) but not different from those of control subjects.

The effects of RV loading abnormality on LV performance are shown in Figure 4, *C* and *D*. Although LV preload was decreased in ASD (decreased EDAI), SAI was well maintained. Ees, Ea, and thus their coupling ratio were comparable with those of normal control subjects.

P-A loops and relations of mild pulmonary stenosis (Figure 4, *D*) were similar to those of normal control sub-

TABLE 2. Hemodynamic characteristics and ventricular-vascular interaction in CHD

	Control	VSD	CoA	ASD	PS
BSA (m^2)	0.7 ± 0.39	0.57 ± 0.34	0.60 ± 0.45	1.1 ± 0.5	0.65 ± 0.46
Heart rate (beats/min)	103.2 ± 13.6	121.0 ± 21.0	113.8 ± 24.5	97.5 ± 9.6	113.8 ± 29.5
SAI (cm^2/m^2)	4.4 ± 0.9	6.2 ± 1.7*	3.6 ± 0.8	4.2 ± 0.9	3.8 ± 2.5
EDAI (cm^2/m^2)	6.7 ± 1.1	10.3 ± 3.2*	6.3 ± 0.4	5.9 ± 1.3*	6.1 ± 3.2
EF (%)	65.5 ± 9.6	62.1 ± 12.2	59.5 ± 10.7	70.4 ± 11.8	62.1 ± 10.5
ESP (mm Hg)	87.8 ± 6.9	84.9 ± 11.9	119.9 ± 32.7*	92.2 ± 13.9	89.1 ± 19.0
dp/dtmax (mm Hg/s)	1611 ± 432	1449 ± 230	1589 ± 263	1816 ± 529	1492 ± 358
Qp/Qs (VSD and ASD)	—	2.3 ± 1.2	—	2.1 ± 0.8	—
ΔP (mm Hg; CoA and PS)	—	—	36.5 ± 16.5	—	37.3 ± 12.5
Msw (mm Hg)	66.4 ± 4.2	54.7 ± 12.7*	77.9 ± 24.9	71.3 ± 17.8	62.3 ± 12.1
Ees (mm Hg · m^2 · cm^{-2})	21.8 ± 7.4	11.6 ± 4.4*	26.7 ± 11.1	23.4 ± 8.6	25.2 ± 8.3
Ao (cm^2/m^2)	–2.3 ± 2.3	–4.7 ± 4.2	–0.9 ± 1.5	–3.8 ± 0.8	–1.2 ± 2.2
Ea (mm Hg · m^2 · cm^{-2})	24.4 ± 8.2	16.4 ± 4.4*	34.3 ± 5.3*	28.9 ± 13.5	28.8 ± 4.9
Ees/Ea	0.91 ± 0.21	0.75 ± 0.28	0.76 ± 0.23	0.87 ± 0.26	0.87 ± 0.21

CHD, Congenital heart disease; *VSD,* ventricular septal defect; *CoA,* coarctation of the aorta; *ASD,* atrial septal defect; *PS,* pulmonary stenosis; *SAI,* stroke area index; *BSA,* body surface area; *EDAI,* end-diastolic area index; *EF,* ejection fraction; *ESP,* end-systolic pressure; *Qp/Qs,* pulmonary/systemic flow ratio; *ΔP,* pressure gradient across the stenotic site; *Msw,* the slope of the stroke work–EDAI relation; *Ees,* end-systolic elastance; *Ao,* intercept; *Ea,* effective arterial elastance.

*$P < .05$ versus control by analysis of variance.

jects. In contrast, LV preload in severe pulmonary stenosis *(lower panel)* was markedly decreased, as indicated by a small EDAI. A steep ESPAR maximized stroke area under this loading condition, suggesting enhanced LV contractility. However, dP/dtmax of this patient was rather small (877 mm Hg/s), mainly because decreased preload and EF (51%) was subnormal as a result of a small stroke area associated with a high heart rate (160 beats/min).

Estimation of ESPAR From a Single Beat

Consistent with the data from a P-V study in adults,[12] $E_N(t_N)$ curves varied relatively little among the patients, particularly early in contraction. This enabled the prediction of Ees from a single P-A loop. Figure 5, *B*, shows a scatter plot of Ees(E_N) versus Ees(MB). The single-beat estimates were the average of results using t_N of 0.25, 0.30, 0.35, and 0.40. These points were selected because of the relatively small variance in the standard $E_N(t_N)$ curve and the stability of Ees calculation at these time points. The variables correlated relatively well, with regression given as Ees(MB) = 0.71Ees(E_N) + 5.8 ($r = 0.75$, $P < .001$). The relationship between Ees(iso) and Ees(MB) is also displayed in Figure 4, *C*. This correlation was also good, with regression given by Ees(MB) = 0.54Ees(iso) + 6.7 ($r = 0.65$, $P < .001$).

Noninvasive Application

Abdominal compression induced increases in EDA in 16 patients (group 1) and decreases in EDA in 12 patients (group 2). The body surface area of group 1 was significantly lower than that of group 2 (0.53 ± 0.3 vs 0.80 ± 0.32 m^2, $P = .04$). Thus, the direction of preload change by abdominal compression apparently depended on body size. Figure 6, *A* and *B*, displays example plots of P-A loops and relations during the ejection period obtained by abdominal compression both at rest (Figure 6, *A*) and under an increased contractile state with dobutamine (Figure 6, *B*) in a representative patient from group 1. The ESPARs on the basis of aortic pressure were similar to those from LV pressure during inferior vena caval occlusion. Figure 6, *C,* shows the baseline correlation between Ees(AO) and Ees(LV). Group 1 patients are indicated by *filled circles* and group 2 patients by *open circles*. Regardless of the direction of preload change ($P = .56$ by means of analysis of covariance), Ees(AO) correlated well with Ees(LV) (Ees[LV] = 1.06 Ees[AO] + 0.34; $r = 0.89$, $P < .01$). Figure 6, *D*, compares changes in Ees [LV] and Ees(AO) caused by dobutamine infusion. ΔEes [AO] provided a reasonable prediction of ΔEes(LV) (ΔEes[LV] = 1.1 ΔEes[AO] + 2.5; $r = 0.81$, $P < .01$). Thus, changes in contractility were accurately estimated by Ees(AO).

Discussion

Traditional evaluation of cardiac function is too often limited by reliance on measurements with complex interdependence between cardiac properties and loading factors.[4,18] P-V relation analysis has evolved as a dominant approach to solve this problem[3,4] and has been widely applied both in experimental[4,19,20] and clinical studies.[21-23] This method is of particular benefit for pediatric patients with CHD, in whom baseline loading conditions are generally abnormal and often change with disease progression or therapeutic intervention.

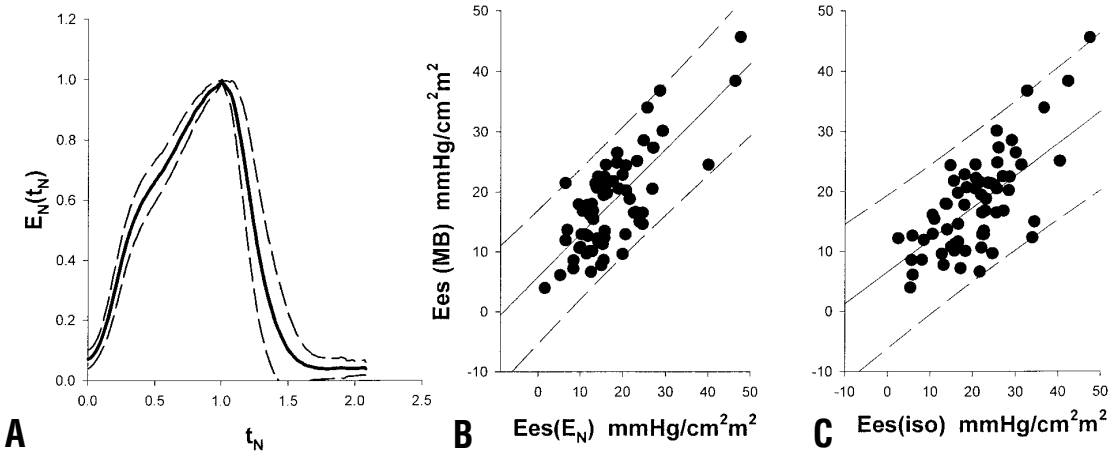

Figure 5. A, Averaged normalized elastance curve ($E_N[t_N]$). Solid lines show means, and dashed lines show ± 1 standard deviation. B, Scatterplot between single-beat estimated Ees on the basis of $E_N(t_N)$ curve (Ees[E_N]) and Ees(MB) during caval occlusion. C, Scatterplot between single-beat estimated Ees by curve fitting (Ees[iso]) and Ees(MB). Linear regression is shown as solid lines; 95% prediction interval is shown as dashed lines.

The present study demonstrated for the first time the applicability of underlying concepts of P-V analysis to various forms of CHD by using P-A analysis. Ventricular area measured by ABD was highly reproducible, and area changes during load manipulation adequately reflected volume changes. The area data combined with pressure recordings provided load-independent measures of contractility, allowing the contractility and loading conditions to be separately quantified. These features of P-A analysis should be of significant clinical value for the cardiovascular assessment of CHD. P-A analysis clarified ventricular contractile states under various loading conditions in CHD, which was not necessarily true of conventional indices because of load dependence. Furthermore, P-A relation analysis could be extended to a simplified and less invasive method. Thus, this approach should provide a useful modality for more detailed assessments of cardiovascular dynamics in pediatric patients with CHD and thereby help in improving the management of patients with this disease.

Area Measurements With ABD in Pediatric Patients With Heart Disease

The conductance catheter[24] enables measurements of instantaneous ventricular volume and has accelerated the application of P-V analysis to human subjects. However, a catheter of the appropriate size for the hearts of infants or small children is not currently available. More important, complex anatomy, particularly that associated with an interventricular communication (including single ventricle), may affect segmental volume determination, making the interpretation of calculated total volume ambiguous. Significant RV volume loading may also affect the LV volume signal during load manipulation.[25] In this regard instantaneous area measurement by ABD has advantages because it can be applied regardless of ventricular morphology or right heart volume. It may also be used in mitral valve regurgitation, where a volume catheter cannot be used because of large signal artifacts.[25] A good example is presented in Figure 2. The conductance catheter cannot be used to construct P-V relations for this complicated ventricle. In addition, ABD has another advantage in that it is far less invasive and complicated compared with a conductance catheter, and it may enable a fully noninvasive P-A analysis, as shown in the present study (Figure 6).

Although area measurement with ABD has many benefits, as noted above, several limitations must be considered. First, there is the potential for lateral translation of the ventricle during varying preloads, resulting in artifactual measurements. However, the linear correlation between changes in stroke area and stroke volume (Figure 1, *B*) suggests that the degree of ventricular translation appeared minimal. Second, the P-A relation may not be applied to a ventricle with regional dysfunction or with abnormal activation, such as a left anterior hemiblock. Little and colleagues[26] reported that pressure-dimension relations can be used to assess global but not regional chamber dysfunction. Although area has an additional dimension and may still reflect volume change of ventricle with mild regional wall motion abnormalities,[27] the quantitative effects of a segmental myocardial abnormality on P-A analysis remain to be elucidated before application to such ventricles.

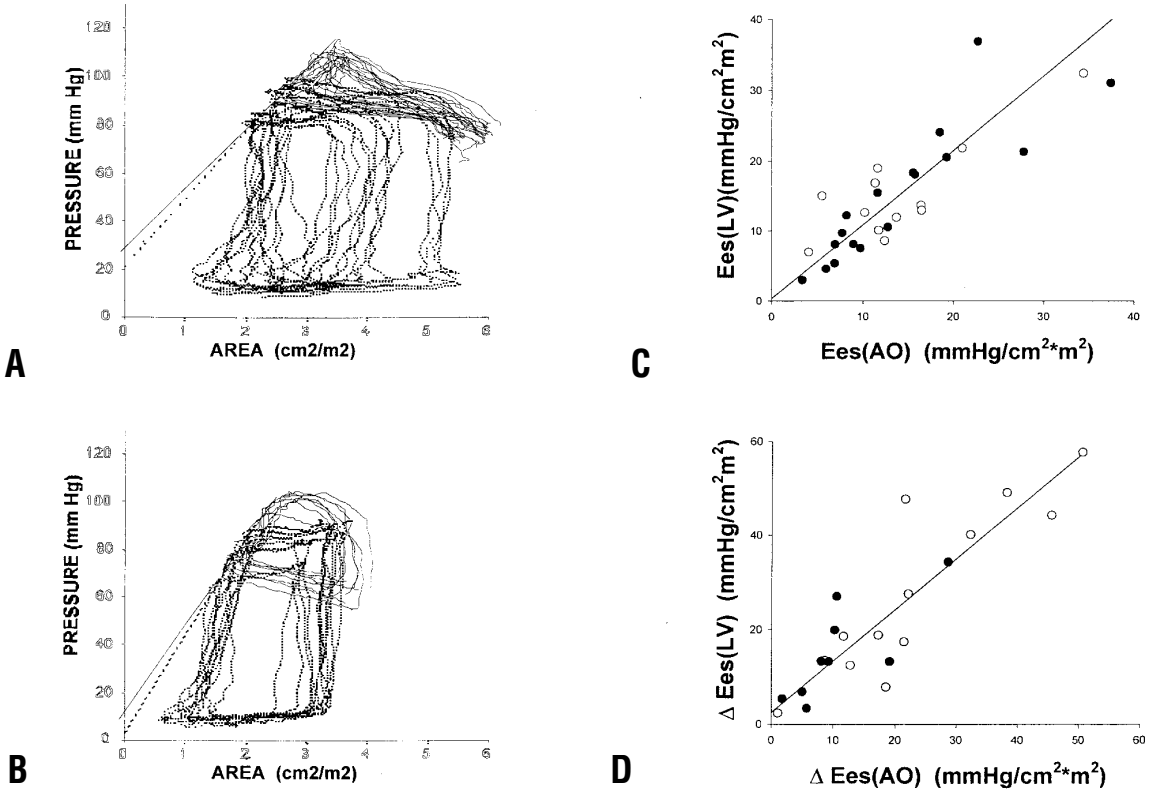

Figure 6. Noninvasive estimation of ESPAR. Example of P-A data before (A) and after (B) dobutamine. P-A loops and relations on the basis of ventricular pressure during caval occlusion are shown by dotted lines and those obtained from aortic pressure during abdominal compression by solid lines. Relations were similar before and after inotropic change. Group data comparing aortic pressure based Ees (Ees[Ao]) versus ventricular pressure–based Ees (Ees[LV]) at baseline (C) and ΔEes(Ao) versus ΔEes(LV) after dobutamine (D).

CHD

Load-insensitive Measures of Contractility

The linear slope of dP/dtmax–end-diastolic volume and stroke work–end-diastolic volume relations, as well as Ees, can be obtained from the same set of P-V data and can characterize relatively load-independent chamber contractility. The present study also demonstrated that similar relations could be obtained by using P-A analysis and that these relations consistently reflected ventricular inotropic change with dobutamine in various forms of CHD. These 3 indices have different levels of sensitivity and stability in the assessment of inotropic changes[28] and should provide more accurate information about chamber contractile states in a compensatory manner.

The adequacy of area measurements with ABD and the behavior of ESPAR with a contractile state presented in this study are consistent with the results of studies conducted in open chest–operated dogs with a transducer placed on the epicardium[29] or in human adults by using transesophageal echocardiography.[30] Our data indicated that P-A analysis is also feasible from the transthoracic approach and applicable even to morphologically abnormal ventricles.

Ventricular-Vascular Coupling

The notable advantage of the concept of P-V analysis is that it provides a description of coupling between the ventricle and the vasculature by independent indices with a common term for chamber and loading properties.[4,31] The present study demonstrated that such features of P-V relation could be conveyed with P-A analysis (Figure 3). This is extremely useful for CHD, where baseline loading conditions are generally abnormal, and pharmacologic or mechanical intervention often alter them significantly. If chamber properties and loading conditions are identified, therapeutic targets can be more clearly focused, and effects from therapeutic intervention can be evaluated more precisely. These should greatly contribute to the improvement of preoperative/postoperative management of patients with CHD.

Ventricular-Vascular Coupling in CHD

By using P-A relations, the present study is the first to reveal basal cardiovascular interaction in various forms of

CHD. The P-A relations clearly characterized diverse LV contractile responses against persistent abnormal loading in association with type and severity, whereas the predominant load dependence of conventional indices confounded such responses.

The LV contractility of ventricular septal defect was rather decreased, despite a normal range of EF. It has been reported that ventricular septal defect is associated with the hypercatecholamic state and that LV contractility is not impaired when assessed by means of EF or circumferential shortening velocity.[32,33] However, the present study revealed that the maintained EF of ventricular septal defect does not necessarily reflect normal contractility but the consequence of decreased afterload resulting from shunt-associated increased stroke volume. This situation may be analogous to that in mitral valve regurgitation, where LV preload is increased and afterload is decreased as a result of increased stroke volume. Nagatsu and colleagues[34] reported that LV contractility measured by using a load-insensitive index was decreased in experimental mitral valve regurgitation, despite preserved EF by increased β-adrenergic support. Because measures of contractility had been shown to be normal, White and Lietman[35] proposed in 1978 that there was no clear rationale for the use of digoxin in patients with ventricular septal defect.[36] Since then, no definite conclusions have been reached in this regard. The results of the present study provide in part supportive evidence for the use of digoxin.

In general, 2 types of clinical manifestation are recognized in patients with coarctation of the aorta.[37] One is in infants with coarctation who present symptoms of heart failure, and the other is in patients who do not present with symptoms as infants but are recognized as children or adolescents with a significant pressure gradient and LV hypertrophy. Our data demonstrated that such differences stemmed from the different LV contractile response to increased afterload. LV contractility increased and matched the afterload in compensated coarctation of the aorta but not in infant-onset coarctation. The P-A diagram predicts that markedly increased afterload inevitably causes a decrease in stroke volume and EF unless Ees increases to a level matching Ea. For example, if the Ees of the patient presented in the lower panel of Figure 4, *B,* increases to produce a similar level of stroke area and EF in the patient presented in the upper panel, then LV peak pressure will rise as high as 160 mm Hg. This may be rather harmful to the LV myocardium of infants. Thus, whether a lack of compensation in symptomatic infants with coarctation of the aorta is due to the protective adaptation of LV or simply the transition from compensation to decompensation is of particular interest, and further studies are needed to clarify this.

LV contractile responses in atrial septal defect and pulmonary stenosis appeared to be dependent mainly on the LV preload reserve. Most patients with atrial septal defect have a left ventricle that is only slightly smaller than normal and are asymptomatic until adulthood, despite a significant left-to-right shunt.[38] The preserved stroke area with normal ventricular-vascular interaction, as shown in Figure 4, *C,* supports this fact. Although mild pulmonary stenosis had minimal effects on LV hemodynamics, as in atrial septal defect, severe pulmonary stenosis significantly limited LV preload, leading to enhanced LV contractility to maintain systemic blood flow.

It is again emphasized that these changes in LV contractility associated with loading alterations were not necessarily delineated by using traditional measures of cardiac function, such as EF or dP/dtmax, because of their predominant load dependence.

Single-Beat Estimation of ESPAR

One important finding of this study was the uniformity of the normalized elastance curve, $E_N(t_N)$, among a variety of CHD types (Figure 5, *A*). This suggests that the time course of ventricular activation is conserved, despite a morphologic and hemodynamic abnormality. This also implies the applicability of time-varying elastance models, the underlying concept of P-V relations, to pediatric patients with CHD and supports the validity of P-A analysis.

In addition to the physiologic insight provided by the consistent $E_N(t_N)$ curve among patients, it also has an important practical implication. With the standard $E_N(t_N)$ curve, Ees could be estimated from a single P-A loop (Figure 5, *B*). A curve-fitting method (E_N[iso]) also provided reasonable estimates of Ees (Figure 5, *C*). These methods are clearly advantageous over complex methods of generating multiple variably loaded cardiac cycles and should enhance their utility. Although these methods yielded reasonable estimates for Ees derived from multiple P-A loops, some estimation errors remained. Introducing adjustments for individual elastance variability[39] or normalizing the amplitude and duration of isovolumic pressure waves[40] may further improve the single-beat method and therefore warrant future studies.

Noninvasive Approach

The present study demonstrated that Ees could be estimated from aortic pressure and ventricular area by using ABD combined with abdominal compression. Central aortic pressure has been estimated with tonometers applied to either the carotid or the subclavian pulse and calibrated with peripheral cuff pressures.[41] Mathematic translation[42] from radial or brachial arterial pressure to central aortic pressure may further facilitate the accurate and easy estimation of central aortic pressure with noninvasive technology. Thus, EAPAR and its coupling to arterial loads (Ea) can be estimated by using a fully noninvasive method. The noninvasive applicability of

P-A analysis not only reduces the risk and burden associated with catheterization, but it could also have wider practical applications. A noninvasive method enables repeated assessments, which could contribute to the earlier detection of disease progression. This is very useful and important for the preoperative and postoperative management of patients with CHD and helps to determine the appropriate timing of catheter-surgical (re)intervention. Furthermore, recording data from large groups of patients not requiring cardiac catheterization is also feasible. This should help reveal cardiovascular (dys)function and improve the management of patients with diseases and conditions not directly associated with heart disease but potentially influencing cardiovascular function, such as diabetes mellitus, growth hormone deficiency, or chemotherapy in malignancy. These studies are currently underway by using tonometry and ABD.

In summary, the present study demonstrated for the first time the applicability of the concept of the P-V framework to pediatric patients with CHD by using ABD-based P-A relations. The methods conveyed all the benefits of P-V analysis and have potential for noninvasive application. Baseline P-A relations varied with the severity and types of loading abnormality in various forms of CHD. This method would help improve the management of pediatric patients with cardiovascular disease.

We thank the medical engineers of Saitama Medical School Hospital for valuable technical assistance in performing the pressure-area studies.

References

1. Graham TP. Ventricular performance in congenital heart disease. *Circulation.* 1991;84:2259-74.
2. Graham TP, Franklin RCG, Wyse RKH, Gooch V, Deanfield JE. Left ventricular wall stress and contractile function in childhood: normal values and comparison of Fontan repair versus palliation only in patients with tricuspid atresia. *Circulation.* 1986;74(Suppl):I-61-9.
3. Suga H, Sagawa K, Shoukas AA. Load independence of the instantaneous pressure-volume ratio of canine left ventricle and effects of epinephrine and heart rate on the ratio. *Circ Res.* 1973;32:314-22.
4. Kass DA, Maughn WL. From Emax to pressure-volume relations: a broader view. *Circulation.* 1988;77:1203-12.
5. Sunagawa K, Maughn WL, Burkhoff D, Sagawa K. Left ventricular interaction with arterial load studied in isolated canine left ventricle. *Am J Physiol.* 1983;245:H773-80.
6. Sunagawa K, Maughn WL, Sagawa K. Optimal arterial resistance for the maximal stroke work studied in isolated canine left ventricle. *Circ Res.* 1985;56:586-95.
7. Suga H. Ventricular energetics. *Physiol Rev.* 1990;70:1203-12.
8. Vandenberg BF, Rath LS, Stuhlmuller P, Melton HE, Skorton DJ. Estimation of left ventricular cavity area with on-line, semiautomated echocardiographic edge detection system. *Circulation.* 1992;86:159-66.
9. Perez JE, Waggoner AD, Barzilai B, Melton HE, Millar JG, Sobel BE. On-line assessment of ventricular function by automatic boundary detection and ultrasonic backscatter imaging. *J Am Coll Cardiol.* 1992;19:313-20.
10. Kono A, Maughn WL, Sunagawa K, Kallman C, Sagawa K, Weisfeldt ML. Left ventricular end-ejection pressure and peak pressure to estimate the end-systolic pressure-volume relationship. *Circulation.* 1984;70:1057-65.
11. Senzaki H, Takayoshi I, Paolocci N, Ekelund U, Hare J, Kass DA. Improved mechanoenergetics and cardiac rest and reserve function of in vivo failing heart by calcium sensitizer EMD-57033. *Circulation.* 2000;101:1040-8.
12. Senzaki H, Chen CH, Kass DA. Single-beat estimation of end-systolic pressure-volume relation in humans: a new method with the potential for noninvasive application. *Circulation.* 1996;94:2497-506.
13. Little WC. The left ventricular dP/dtmax-end-diastolic volume relation in closed-chest dogs. *Circ Res.* 1985;56:808-15.
14. Glower DD, Spratt JA, Snow ND, Kabas JS, Davis JW, Olsen CO, et al. Linearity of the Frank-Starling relationship in the intact heart: the concept of preload recruitable stroke work. *Circulation.* 1985;71:994-1009.
15. Sunagawa K, Yamada A, Senda Y, Kikuchi Y, Nakamura M, Shibahara T, et al. Estimation of the hydromotive source pressure from ejecting beats of the left ventricle. *IEEE Trans Biomed Eng.* 1980;27:299-305.
16. Takeuchi M, Igarashi Y, Tomimoto S, Odake M, Hayashi T, Tsukamoto T, et al. Single-beat estimation of the slope of the end-systolic pressure-volume relation in the human left ventricle. *Circulation.* 1991;83:202-12.
17. Takata M, Wise RA, Robotham JL. Effects of abdominal pressure on venous return: abdominal vascular zone conditions. *J Appl Physiol.* 1990;69:1961-72.
18. Kass DA, Maughn WL, Gui AM, Kono A, Sunagawa K, Sagawa K. Comparative influence of load versus inotropic states on indexes of ventricular contractility: experimental and theoretical analysis based on pressure-volume relationships. *Circulation.* 1987;76:1422-36.
19. Senzaki H, Gluzband YA, Pak PH, Crow MT, Janicki JS, Kass DA. Synergistic exacerbation of diastolic stiffness from short-term tachycardia-induced cardiodepression and angiotensin II. *Circ Res.* 1998;82:503-12.
20. Georgakopoulos D, Mitzner WA, Chen CH, Byrne BJ, Millar HD, Hare JM, et al. In vivo murine left ventricular pressure-volume relations by miniaturized conductance micromanometry. *Am J Physiol.* 1998;274:H1416-22.
21. Senzaki H, Fetics B, Chen CH, Kass DA. Comparison of ventricular pressure relaxation assessments in human heart failure: quantitative influence on load and drug sensitivity analysis. *J Am Coll Cardiol.* 1999;34:1529-36.
22. Pak PH, Maughn WL, Baughman KL, Kass DA. Marked discordance between dynamic and passive diastolic pressure-volume relations in idiopathic hypertrophic cardiomyopathy. *Circulation.* 1996;94:52-60.
23. Kass DA, Chen CH, Curry C, Talbot M, Berger R, Fetics B, et al. Improved left ventricular mechanics from acute VDD pacing in patients with dilated cardiomyopathy and ventricular conduction delay. *Circulation.* 1999;99:1567-73.
24. Baan J, van der Velde E, de Bruin H, Smeenk G, Keeps J, van Dijk A, et al. Continuous measurement of left ventricular volume in animals and man by conductance catheter. *Circulation.* 1984;70:812-23.
25. Kass DA, Yamazaki T, Burkhoff D, Maughn WL, Sagawa K. Determination of left ventricular end-systolic pressure-volume relationships by the conductance (volume) catheter technique. *Circulation.* 1986;73:586-95.
26. Little WC, Freeman GL, O'Rourke RA. Simultaneous determination of left ventricular end-systolic pressure-volume and pressure-dimension relationships in closed-chest dogs. *Circulation.* 1985;71:1301-8.
27. Gorcsan J, Gasior TA, Mandarino WA, Deneault LG, Hattler BG, Pinsky MR. On-line estimation of changes in left ventricular stroke volume by transesophageal echocardiographic automated border detection in patients undergoing coronary artery bypass grafting. *Am J Cardiol.* 1993;72:721-7.
28. Little WC, Chen CP, Mumma M, Igarashi Y, Vinten-Johansen J, Johnston WE. Comparison of measures of left ventricular contractile performance derived from pressure-volume loops in conscious dogs. *Circulation.* 1989;80:1378-87.
29. Gorcsan J, Romand JA, Mandarino WA, Deneault LG, Pinsky MR. Assessment of left ventricular performance by on-line pressure-area relations using echocardiographic automated border detection. *J Am Coll Cardiol.* 1994;23:242-52.
30. Gorcsan J, Gasior TA, Mandarino WA, Deneault LG, Hattler BG, Pinsky MR. Assessments of the immediate effects of cardiopulmonary

bypass on left ventricular performance by on-line pressure-area relations. *Circulation.* 1994;89:180-90.
31. Kass DA, Grayson R, Marino P. Pressure-volume analysis as a method for quantifying simultaneous drug (amrinone) effects on arterial load and contractile state in vivo. *J Am Coll Cardiol.* 1990;16:726-32.
32. Sahn DJ, Vaucher Y, Williams DE, Allen HD, Goldberg SJ, Friedman WF. Echocardiographic detection of left-to-right shunts and cardiomyopathies in infants and children. *Am J Cardiol.* 1976;38:73-9.
33. Baylen B, Meyer RA, Korfhangen J, Benzing G 3rd, Bubb ME, Kaplan S. Left ventricular performance in the critically ill premature infant with patent ductus arteriosus and pulmonary disease. *Circulation.* 1977;55:182-8.
34. Nagatsu M, Zile MR, Tsutsui H, Schmid PG, DeFreyte GD, Cooper G, et al. Native β-adrenergic support for left ventricular dysfunction in experimental mitral regurgitation normalizes indexes of pump and contractile function. *Circulation.* 1994;89:818-26.
35. White RD, Lietman PS. A reappraisal of digitalis for infants with left-to-right shunts and heart failure. *J Pediatr.* 1978;92:867-9.
36. Alpert BS, Barfield JA, Taylor WJ. Reappraisal of digitalis in infants with left-to-right shunts and heart failure. *J Pediatr.* 1985;106:66-8.
37. Graham TP. Congenital heart disease. In: Macartney FJ, ed. Ventricular function in congenital heart disease. Lancaster, United Kingdom: MTP Press; 1986. p. 142-162.
38. Graham TP, Jarmakani JM, Canent RV. Left heart volume characteristics with a right ventricular volume overload: total anomalous pulmonary venous connection and large atrial septal defect. *Circulation.* 1972;45:389-96.
39. Fetics BJ, Nevo E, Nakayama M, Wong EY, Pak PH, Maughn WL, et al. Total non-invasive estimation of left-ventricular end-systolic elastance from steady-state data. *Circulation.* 1997(Suppl):I-640-96.
40. Regen DM, Howe WC, Peterson JT, Little WC. Characteristics of single isovolumic left-ventricular pressure waves of dog hearts in situ. *Heart Vessel.* 1993;8:136-48.
41. Kelly R, Hayward C, Ganis J, Daley J, Avolio A, O'Rourke M. Noninvasive registration of the arterial pressure waveform using high fidelity applanation tonometry. *J Vasc Med Biol.* 1989;1:142-149.
42. Chen CH, Nevo E, Fetics B, Pak PH, Yin FC, Maughan WL, et al. Estimation of central aortic pressure waveform by mathematical transformation of radial tonometry pressure: validation of generalized transfer function. *Circulation.* 1997;95:1827-36.

Appendix 1

By definition, Ees and Ea can be described as follows:

$$Ees = ESP/(ESA - Ao) = ESP/(ADA - SA - Ao) \quad (1)$$

$$Ea = ESP/SA \quad (2)$$

where ESP is end-systolic pressure, ESA is end-systolic area, and SA is stroke area.

Combining equations 1 and 2 yields the following:

$$SA = Ees(EDA - Ao)/(Ea + Ees) \quad (3)$$

where EDA is end-diastolic area. Thus,

$$EF = SA/EDA = Ees[1 - (Ao/EDA)]/(Ea + Ees) \quad (4)$$

Appendix 2

Time-varying elastance (E[t]) was defined as the instantaneous ratio of $P(t)/[A(t) - A_o]$, where P(t) and A(t) are ventricular pressure and area at time t. The maximal value of E(t) (E_{max}) and the time to achieve E_{max} referenced from the R wave of the electrocardiogram (t_{max}) were both determined. The normalized E(t) function was then defined as follows:

$$E_N(t_N) = E(t_N)/E_{max} \quad (5)$$

where

$$t_N = t/t_{max} \quad (6)$$

To combine $E_N(t_N)$ relations, each curve was resampled at 200 equispaced intervals by using linear interpolation, and the results were averaged, yielding a standard $E_N(t_N)$ curve.

Appendix 3

Chamber elastance at time t_N was as follows:

$$E(t_N) = P(t_N)/[A(t_N) - A_o] \quad (7)$$

Elastance at time t_{max} was as follows:

$$E(t_{max}) = E_{max} = P(t_{max})/[V(t_{max}) - A_o] \quad (8)$$

From equation 5, the ratio of $E(t_N)/E_{max}$ equaled $E_N(t_N)$. Thus, combining equations 5, 7, and 8 yielded the following:

$$A_o = [P_N(t_N) \times A(t_{max}) - A(t_N) \times E_N(t_N)]/[P_N(t_N) - E_N(t_N)] \quad (9)$$

where $P_N(t_N) = P(t_N)/P(t_{max})$. Once A_o was calculated, E_{max} was determined from equation 8. This E_{max} value was referred to as $Ees(E_N)$.

Appendix 4

For each steady-state beat, pressure data between end-diastolic pressure and dP/dtmax and between dP/dtmin and the point at which pressure declined to end-diastolic pressure were fit by means of nonlinear regression to the following formula:

$$P(t) = 0.5 \times P_{iso} \times [1 - \cos(\omega t + \phi)] + EDP \quad (10)$$

where EDP was end-diastolic pressure and P_{iso} was the estimated peak isovolumic pressure. Ees (Ees[iso]) was then calculated from the following:

$$Ees(iso) = [P_{iso} - ESP]/[EDA - ESA] \quad (11)$$

CHD